NANOCOMPOSITES: RADIATIVE GASIFICATION AND VINYL POLYMER FLAMMABILITY

by

J.W. Gilman, Takashi Kashiwagi
and S. Lomakin
Building and Fire Research Laboratory
National Institute of Standards and Technology
Gaithersburg, MD 20899, USA
and
E.P. Giannelis and E. Manias
Cornell University
Ithaca, NY, USA
and
J.D. Lichtenhan, P. Jones
Air Force Research Laboratory
Edwards Air Force Base, CA, USA

Reprinted from the 6th European Meeting on Fire Retardancy of Polymeric Materials (FRPM'97), September 24-26, 1997. Organised jointly by the 'Laboratoire de Chimie Analytique et de Physico-Chimie des Solides' de l'E.N.S.C. de Lille and the 'Centre de Recherche et d'Etude des Procédés d'Ignifugation des Matériaux' at her University of Lille (France). Proceedings. Special Publication No. 224. The Royal Society f Chemistry, Thomas Graham House, Science Park, Milton Road, Cambridge CB4 4WF, UK, 1998.

NANOCOMPOSITES:
RADIATIVE GASIFICATION AND VINYL POLYMER FLAMMABILITY.

J. W. Gilman, Takashi Kashiwagi

National Institute of Standards and Technology
Gaithersburg, MD, USA

E. P. Giannelis and E. Manias

Cornell University
Ithaca, NY, USA

S. Lomakin

Guest Researcher at NIST
from the Russian Academy of Sciences, Moscow, Russia.

J. D. Lichtenhan, P. Jones

Air Force Research Laboratory, Edwards Air Force Base, CA, USA

In the pursuit of improved approaches to flame retarding polymers a wide variety of concerns must be addressed. The low cost of commodity polymers requires that the fire retardant (FR) approach be of low cost. This limits the solutions to the problem primarily to additive type approaches. These additives must be easily processed with the polymer, must not excessively degrade the other performance properties, and must not create environmental problems in terms of recycling or disposal. Currently, some of the commonly used flame retardant approaches for polymers can reduce the thermal and mechanical properties of the polymer[1-3]. Polymer-clay nanocomposites are hybrid organic polymer inorganic layered materials with unique properties when compared to conventional filled polymers. The mechanical properties for nylon-6 clay nanocomposite, with clay mass fraction of 5 %, show excellent improvement over those for the pure nylon-6. The nanocomposite exhibits a 40 % higher tensile strength, 68 % greater tensile modulus, 60 % higher flexural strength, 126 % increased flexural modulus, and comparable impact strengths. The heat distortion temperature (HDT) is increased from 65°C to 152°C[4]. Previously, we reported on the flammability properties of nylon-6 clay nanocomposites[5]. Here, we will briefly review these results, present the results of radiative gasification experiments and report on our initial studies of the flammability of

intercalated polymer-clay nanocomposites prepared from polystyrene, PS, and polypropylene-graft-maleic anhydride, PP-g-MA.

1. EXPERIMENTAL

1.1. Cone Calorimeter

Evaluations of flammability were done using the Cone Calorimeter[6]. The tests were done at an incident heat flux of 35 kW/m^2 and 50 kW/m^2, using a cone shaped heater. A heat flux of 35 kW/m^2 represents a typical small-fire scenario[7]. Peak heat release rate, mass loss rate and specific extinction area data, measured at 35 kW/m^2, are reproducible to within ± 15 %. The carbon monoxide and heat of combustion data are reproducible to within ± 10 %. The uncertainties for the Cone calorimeter are based on the uncertainties observed while evaluating the thousands of samples combusted to date. Typically two samples were combusted in each case in the Cone, and the results averaged. Cone samples were prepared by compression molding the samples (20g to 50g) into rectangular or round plaques, 4mm to 15 mm thick, with a typical area of ~ 0.004 m^2, using a press with a heated mould.

1.2. Radiative Gasification

Figure 1 shows a gasification apparatus which is similar to the Cone calorimeter. The gasification apparatus allows pyrolysis, in a nitrogen atmosphere, of samples identical to those used in the Cone calorimeter, at heat fluxes like those experienced in a fire (30 kW/m^2 to 100 kW/m^2). It allows study of the condensed phase decomposition processes decoupled from the gas phase combustion and resulting heat feedback from the flame. In a typical experiment thermocouples are imbedded in the sample to monitor the temperature at which the pyrolysis and decomposition processes occur. A load cell gives mass loss rate data which can be compared to mass loss rate data from the Cone calorimeter experiments. A video camera records the pyrolysis and charring phenomena.

1.3. Nylon-6 clay nanocomposites

Nylon-6 clay nanocomposites (clay mass fraction of 2 % and 5 %) and nylon-6 were obtained from UBE industries and used as received.[8] The above nanocomposites will be referred to as nylon-6 clay nanocomposite (2%) and nylon-6 clay nanocomposite (5%), respectively.

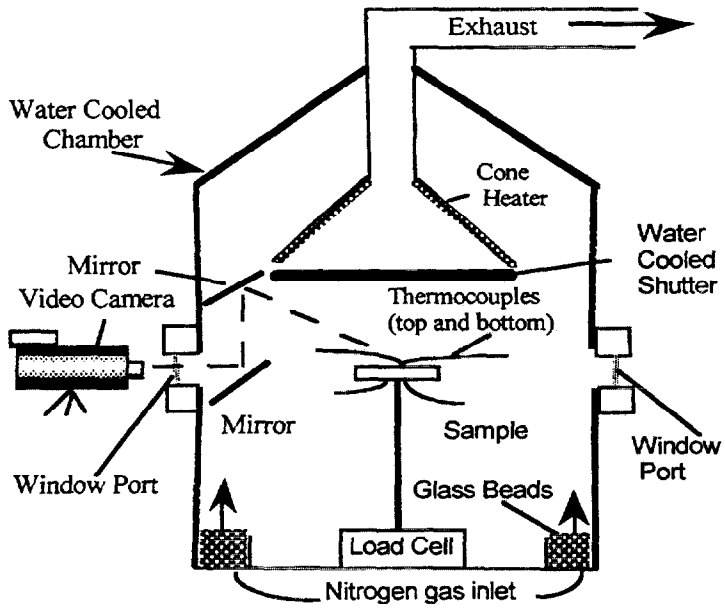

Figure 1. *A schematic of the radiative gasification apparatus (1 m diameter, 2 m height). The gasification apparatus allows pyrolysis, in a nitrogen atmosphere, of samples identical to those used in the Cone calorimeter.*

1.4. PS-clay-nanocomposite

Preparation of PS-clay-nanocomposite (clay mass fraction of 3 %) by melt blending PS with bis(dimethyl)bis(octadecyl)ammonium-exchanged montmorillonite, yields a nanocomposite with the *intercalated* structure (see Scheme 1). The inter-gallery spacing, by X-ray diffraction, XRD, is 3.1 nm ($2\theta = 2.7$). In the *intercalated* form and at this low clay concentration this nanocomposite is essentially a blend, with *intercalated*-PS-clay domains dispersed in pure PS. The *immiscible* PS-clay mix, where the clay is only mixed in at the primary-particle size scale (~5 μm), is prepared under the same melt blending conditions except the alkylammonium used to compatibilize the montmorillonite has only one octadecyl R group instead of two. This renders the ion exchanged montmorillonite slightly less organophilic and intercalation does not occur. These PS-clay combinations will be referred to as *intercalated*-PS-clay (3 %) nanocomposite and *immiscible* PS-clay (3 %) mixture. The PS used was Styron 6127 from Dow Chemical Co.

1.5. PP-g-MA-clay-nanocomposite

Preparation of PP-g-MA-clay-nanocomposite (clay mass fraction of 5 %) by melt blending was accomplished by pressing the PP-g-MA mixed with the bis(dimethyl)bis(tallow)ammonium-exchanged montmorillonite, Closite 15A, at 160°C for 30 minutes using a Carver press, followed by heating in a vacuum oven for several hours at 160°C. This yields a nanocomposite with the *intercalated* structure (see scheme 1). The inter-gallery spacing, by XRD analysis, is 3.6 nm. PP-g-MA (m.p.: 152°C) was purchased from Aldrich and contains a mass fraction of 0.6 % maleic anhydride. It has a melt index of 115 g / 600 s, a Mw of ~ 10K and Mn ~ 5K.

1.6. Characterisation

X-ray diffraction spectra were collected on a Phillips diffractometer using Cu Kα radiation, (λ= 0.1505945 nm). Powder samples were ground to a particle size of less than 40 μm. Solid polymer-clay monoliths were typically 14 mm by 14 mm with a 2 mm thickness.

Thermogravimetric analysis, TGA, was done on a Perkin-Elmer 7 Series TGA. Four runs of each sample type were typically run, the results averaged and the uncertainties calculated using standard methods. The samples were heated from 30°C to 600°C at a heating rate of 10°C/ minute in a nitrogen atmosphere. For the differential TGA plots (Figure 10) the uncertainty in the maximum of the mass loss rate ($d(m/m_0)/dT$ ($°C^{-1}$)), in the normalised mass loss rate versus temperature plots, was found to be ± 20 % (± 1 standard deviation). The uncertainty in the temperature at the maximum, in the normalised mass loss rate versus temperature plots, was found to be ± 2 % (± 1 standard deviation).

TGA-FTIR was performed on a TA Instruments (Model TGA-951) TGA coupled to a FTIR gas analyser manufactured by Nicolet Inc. (Model 7-SX). Samples (5 mg - 10 mg) were first flushed with nitrogen at 100 cm^3/minute for 30 minutes and then heated at 10°C/minute from room temperature (25°C) to 1000°C under nitrogen. Evolved gases from the sample were swept through a heated (250°C) capillary transfer line to a gas analysis cell and then to the spectrometer sample compartment by nitrogen purge gas. FTIR spectra were recorded once every 6 s at resolution of 8 cm^{-1}.

Transmission electron microscopy (TEM), the char was broken into small pieces, embedded in an epoxy resin (Epofix), and cured overnight at room temperature. Ultra-thin sections were prepared with a 45° diamond knife at room temperature using a DuPont-Sorvall 6000

ultramicrotome. Thin sections (nominally 50 nm-70 nm) were floated onto water and mounted on 200-mesh carbon-coated copper grids. Bright-field TEM images were obtained with a Philips 400T microscope operating at 120 kV, utilising low-dose techniques.

2. BACKGROUND

The polymer-clay nanocomposites contain montmorillonite clay that has had the sodium ions removed by ion-exchange with various alkyl ammonium salts. This modification renders the usually hydrophilic clay organophilic. A molecular representation of the layered structure of sodium montmorillonite is shown in Figure 2.

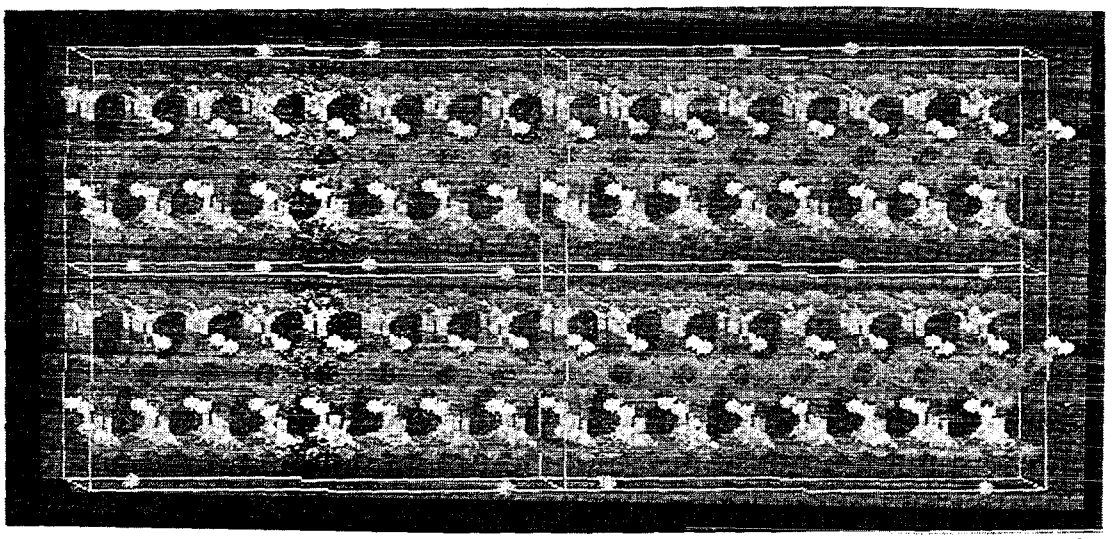

Figure 2. *Molecular representation of sodium montmorillonite, showing two aluminosilicate layers with the Na^+ cations in the interlayer gap or gallery (1.14 nm spacing between layers).*

The nylon-6 clay nanocomposites are synthesised by ring-opening polymerization of ε-caprolactam in the presence of cation exchanged montmorillonite clay[9]. This process creates a polymer layered silicate nanocomposite with either a *delaminated* structure or an *intercalated* structure (see Scheme 1), depending on the clay content. The *intercalated* structure, which forms when the mass fraction of clay is greater than 20 %, is characterized by a well ordered multilayer with spacing between the silicate layers (gallery spacing) of only a few nanometers. The *delaminated* structure, which forms when the mass fraction of clay is less than 20 %, contains the silicate layers individually dispersed in the polymer matrix. The *delaminated* structure is less ordered and the gallery spacing is greater, 10 nm to 100 nm.

3. FLAMMABILITY STUDIES

3.1 Nylon-6 clay nanocomposite

To evaluate the feasibility of controlling polymer flammability via a nanocomposite approach, we examined the flammability properties, using the Cone calorimeter, of nylon-6 clay nanocomposites and compared them to those for pure nylon-6. The Cone calorimeter data, shown in Figure 3, indicates that the peak heat release rate (HRR), an important parameter for predicting fire hazard[10], is reduced by 63 % in a nylon-6 clay-nanocomposite containing a clay mass fraction of only 5 %. These samples were exposed to a heat flux of 35 kW/m^2.

This reduction in HRR is comparable to that found for commercial flame retarded (FR) polymers, but at a lower mass fraction of "additive" than is typical (see Table 1). This system maintains effectiveness even at higher heat fluxes. The peak HRR is reduced by 68 % when the samples are exposed to a heat flux of 50 kW/m^2. From the Cone calorimeter data the nanocomposites were found to have the same heat of combustion as the pure nylon-6. Furthermore, the nanocomposites did not increase the rate of carbon monoxide or soot (measured by the specific extinction area, SEA) formation during the combustion, as some flame retardants do[11,12]. Figure 4 shows the mass loss rate data for nylon-6, and nylon-6 clay-nanocomposite (5 %). The two curves closely resemble the HRR curves, indicating that the reduction in HRR for the nanocomposites is primarily due to the reduced mass loss rate and the resulting lower fuel feed rate to the gas phase. This data indicates that the nano-dispersed clay modifies the condensed phase and not the gas phase processes of the polymer during the combustion.

We did not find the same behavior (i.e., reduced mass loss rate) when we studied the milligram scale thermal properties of these materials. We found that the nylon-6 nanocomposite had the same thermal decomposition behavior when the thermal stability was probed using thermogravimetric analysis combined with Fourier transform infrared spectroscopy, TGA-FTIR. The peak of the derivative of the mass loss versus time curves were both at 460°C ± 10°C. The FTIR data for both samples were identical and corresponded to the spectrum for ε-caprolactam with traces of CO and CO_2. The TGA-residue yields were 0.3 wt. % (± 0.1 wt. %) for nylon-6 and 5.5 mass % (± 1.0 wt. %) for the nanocomposite.

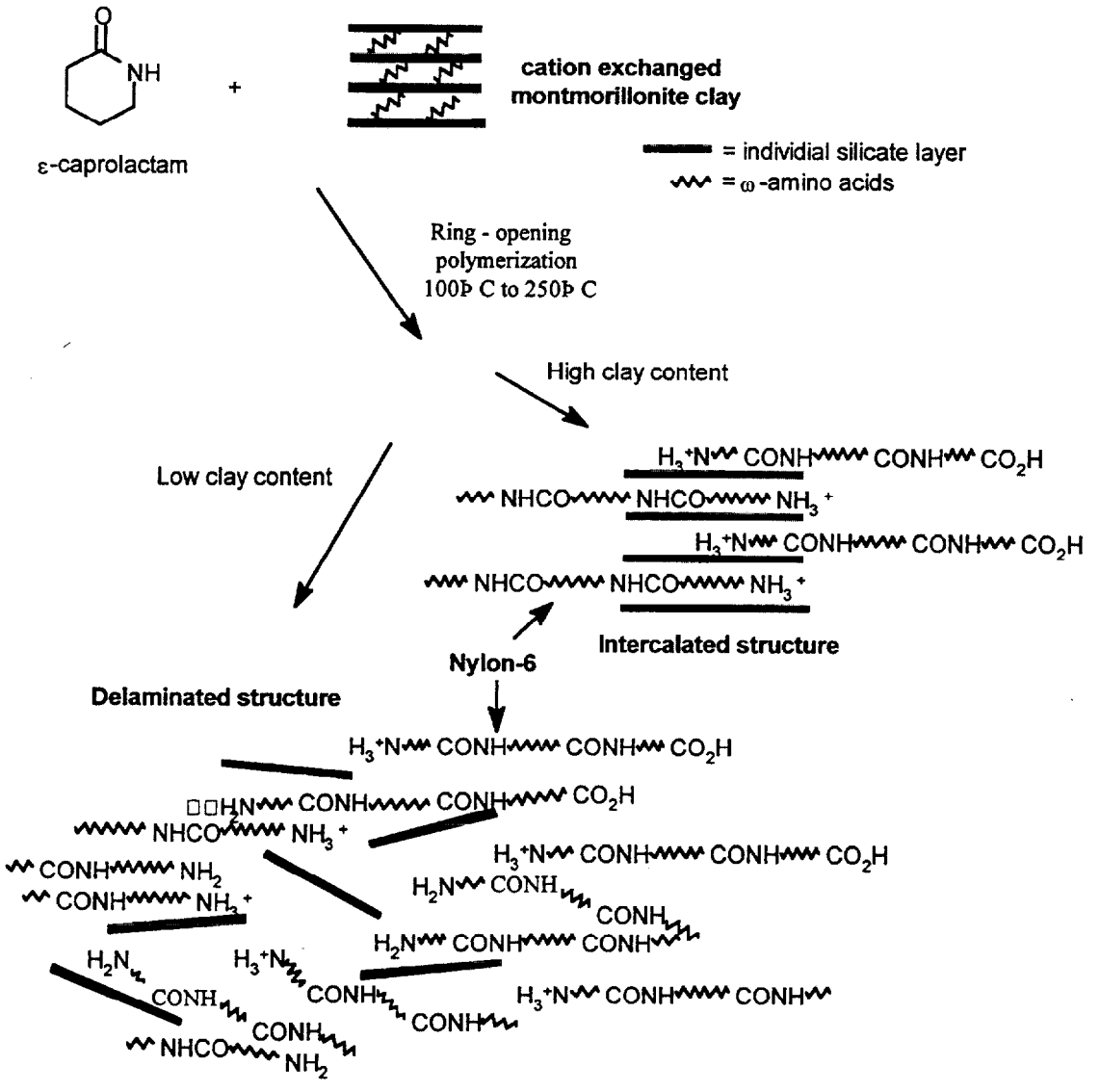

Scheme 1. *Diagram of the process used to prepare polymer layered silicate nanocomposites with either a delaminated structure or an intercalated structure.*

After accounting for the amount of clay present (5 wt. %) in the nanocomposite, these carbonaceous residue yields are essentially the same. This was somewhat surprising since other studies of the thermal reactions in layered organic-clay intercalates, at 400°C, reported formation of carbonaceous-clay residues and other condensation and crosslinking type reaction products[13]. These data indicate that the mechanism of flame retardancy is not via retention of a large fraction of carbonaceous char in the condensed phase.

Visual observations of the combustion experiments, in the Cone calorimeter, reveal different behavior for the nylon-6 clay-nanocomposites, compared to the pure nylon-6. A thin char layer forms, on the top of all the samples, in the first few minutes of exposure, prior to ignition. In the case of pure nylon-6, this char layer fractures into small pieces early in the combustion. The char does not fracture with the nylon-6 clay-nanocomposites. This tougher char layer survives and grows throughout the combustion, yielding a rigid multicellular char-brick with somewhat larger dimensions as compared to the original sample.

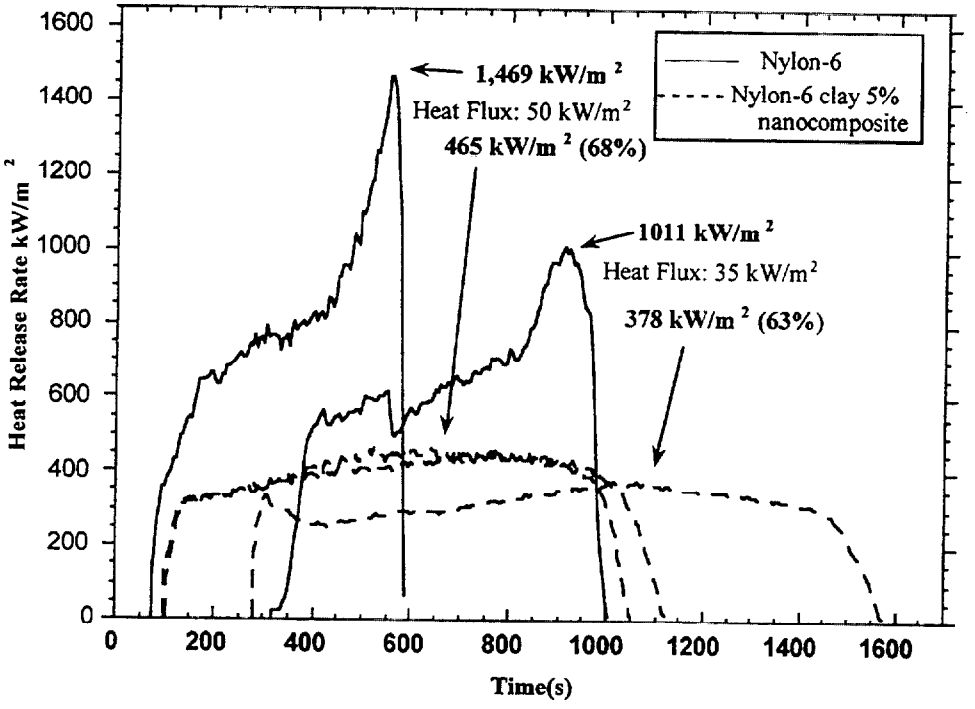

Figure 3. *Heat release rate versus time plot for nylon-6 clay-nanocomposite (5 mass %) and pure nylon-6. The data for the 35 kW/m² and 50 kW/m² flux exposures are shown. Two experiments at the 50 kW/m² flux exposure are included to show the typical reproducibility. The nanocomposite has a 63 % lower HRR at 35 kW/m² and a 68 % lower HRR at 50 kW/m².*

We proposed that the *delaminated* hybrid structure collapses as the nylon-6 decomposes. This forms a reinforced char layer which acts as an insulator and a mass transport barrier, slowing the escape of the volatile products (e.g. ε-caprolactam) generated as the nylon-6 decomposes. Indeed, transmission electron microscopy (TEM) of a section of the char-residue from the combustion of the nylon-6 clay-nanocomposite, shown in Figure 5,

reveals a multilayered-silicate structure. X-ray diffraction, XRD, shown in Figure 6, and TEM give an interlayer spacing of 1.3 nm ($2\theta = 6.9°$).

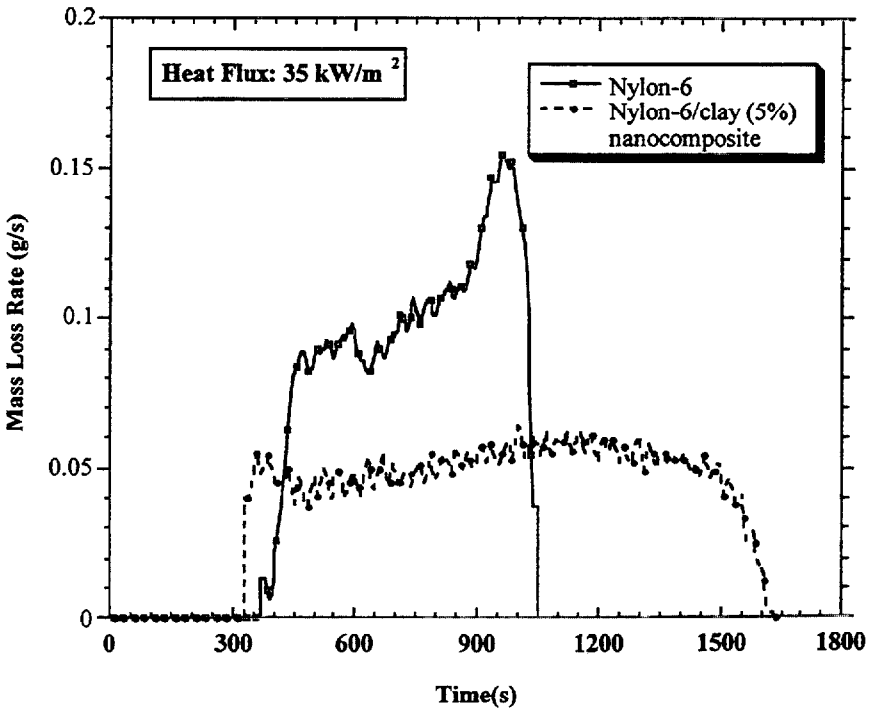

Figure 4. *The mass loss rate data for nylon-6, and nylon-6 clay-nanocomposite (5 %).*

XRD also shows a peak for the 0.33 nm spacing between layers in graphitic-carbon ($2\theta = 26.7°$). The carbon presumably occupies the interlayer space between the silicate layers. The nanocomposite structure of the char appears to enhance the performance of the char, just as the nanocomposite structure enhances the performance of the nylon-6. Since the nanocomposites have excellent barrier properties, an additional effect, due to the low permeability of liquids and gases through the nylon-6 nanocomposite char-residue, may also be responsible for the slow transport of volatile fuel to the gas phase[14]. Recent molecular dynamics simulations of the thermal degradation of nano-confined polypropylene support this type of mechanistic hypothesis[15].

4 RADIATIVE GASIFICATION

4.1 Nylon-6 clay nanocomposite

Figure 1 shows the gasification apparatus. The gasification apparatus allows pyrolysis, in a

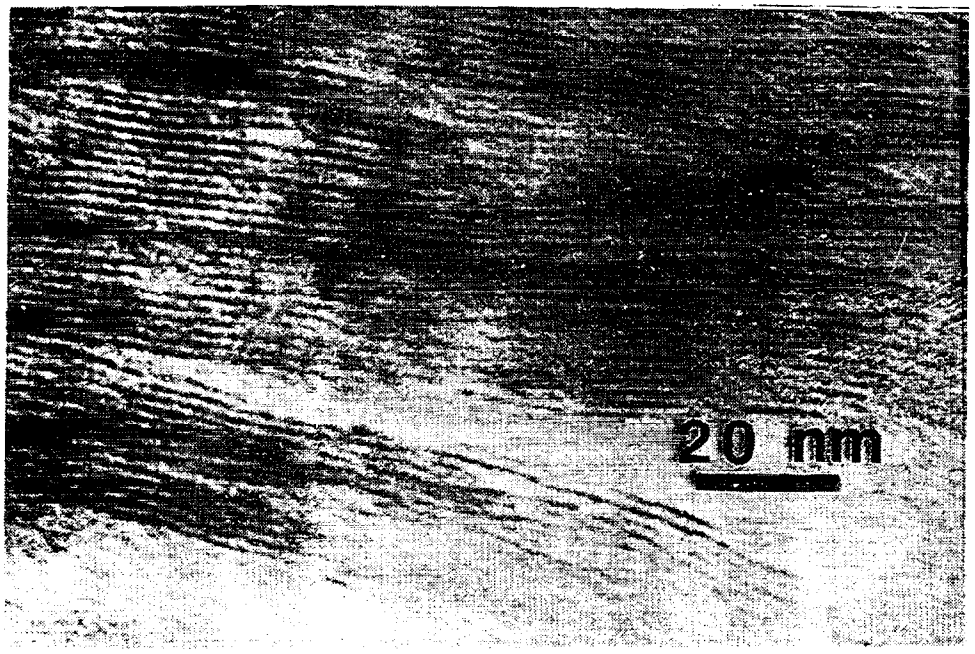

Figure 5. *TEM of a section of the combustion char from the nylon-6 clay-nanocomposite (5 %) showing the silicate (1 nm thick, dark bands) multilayered structure. This layer may act as an insulator and a mass transport barrier.*

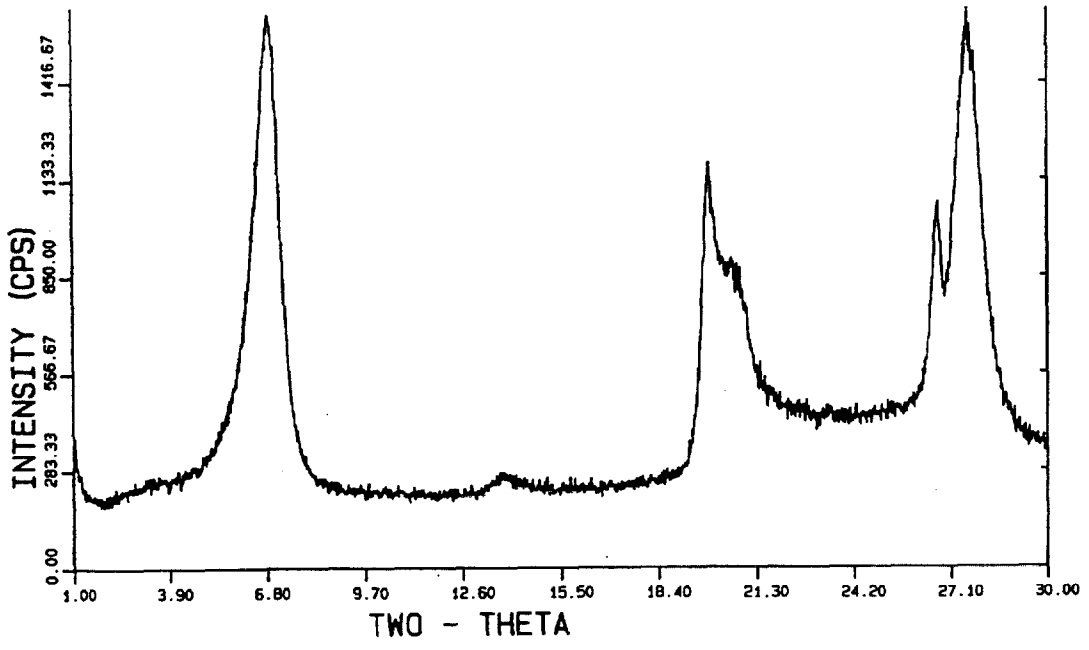

Figure 6. *X-ray diffraction pattern of the char residue from combustion of nylon-6-clay nanocomposite in the Cone calorimeter. This gives an interlayer spacing for the clay in the char residue of 1.3 nm ($2\theta = 6.9°$).*

nitrogen atmosphere, of samples identical to those used in the Cone calorimeter. Figure 7 shows the mass loss rate curves for a set of experiments, carried out in the gasification apparatus, aimed at comparing the pyrolysis behavior of the nanocomposite to that for pure nylon-6. The slope of the mass loss curve for the nanocomposite significantly differs from that for the pure nylon-6 at ~ 180 seconds. The digitized video images, shown in Figure 8, of the pyrolysis experiments, reveal that the nanocomposite (center column) begins to char at the edges of the sample at 120 seconds. The thermocouple on the bottom of the sample shows that the temperature, at 240 seconds, is ~ 50°C to 75°C lower, under the nanocomposite sample, than under the pure nylon-6 sample. These images also show that the formation of a char layer on the top of the nanocomposite sample (center column) occurs at the same time, 180 seconds, that the mass loss rate of the sample slows. Presumably it is this char layer that is responsible for both the lower back-side temperature and the lower mass loss rate for the nylon-6 nanocomposite. Figure 8 also shows the effect of oxygen on the charring process for the nylon-6 nanocomposite. The images in the column on the right are of the pyrolysis of the nylon-6 nanocomposite in a nitrogen - oxygen atmosphere with an oxygen volume fraction of 7.5 %. It appears that the presence of oxygen causes the charring process to occur earlier in the pyrolysis. Even at 60 seconds the entire sample is darkened and at 120 seconds most of the surface is charred.

This is similar to the pre-ignition charring, mentioned above, for the nanocomposite in the Cone experiment. However the mass loss rate for the nylon-6 nanocomposite is not significantly different in the oxygenated pyrolysis atmosphere. The residue yields are also the same (5.0 wt. % ± 0.5 wt. %) within the experimental uncertainty. Comparison of the mass loss data from the Cone calorimeter experiment (Figure 4) to the mass loss data from the gasification experiment (Figure 7), shows that the nanocomposite has a lower mass loss rate in the Cone than in the gasification apparatus. In the Cone calorimeter, the mass loss rate for the nanocomposite, is 62 % lower than the mass loss rate for nylon-6. In the gasification apparatus, the mass loss rate for the nanocomposite, is only 35 % lower than the mass loss rate for nylon-6. Some of this difference is due to the fact that in the Cone a sample with a lower HRR experiences a reduced heat feed back (~ 10 kW/m^2) from the flame and hence is exposed to a lower net flux.

This further reduces the HRR and the mass loss rate. This does not occur in the gasification experiment. Each sample is exposed to the same flux throughout the pyrolysis.

Some of this effect may be due to the effect of oxygen on the mechanism of flame retardancy for the nanocomposite.

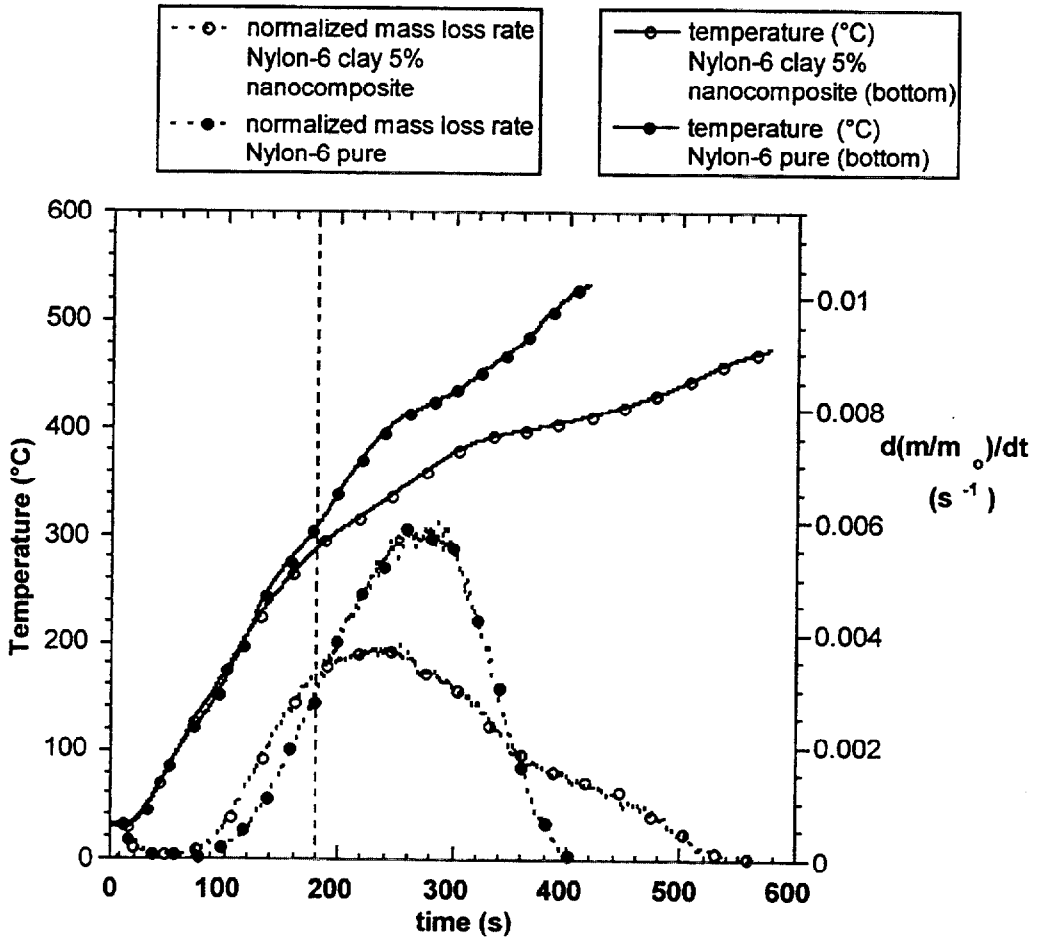

Figure 7. *Normalized Mass loss rate and temperature versus time plots for the gasification experiments for nylon-6 and nylon-6 clay (5%) nanocomposite with N_2 atmosphere. All samples were exposed to a flux of 40 kW/m^2 in a N_2 atmosphere. The mass loss rate curves begin to differ at 180 seconds when the surface of the nanocomposite sample is partially covered by char.*

Another difference was also observed for the nanocomposites between the Cone results and the gasification results. Although the residue yields for both experiments are the same (~5.5 wt. %), the volume of the residue from the Cone sample is several times greater than that from the gasification sample. Recall that above we mentioned the formation of a rigid multicellular char-brick with the same or somewhat larger dimensions as the original sample.

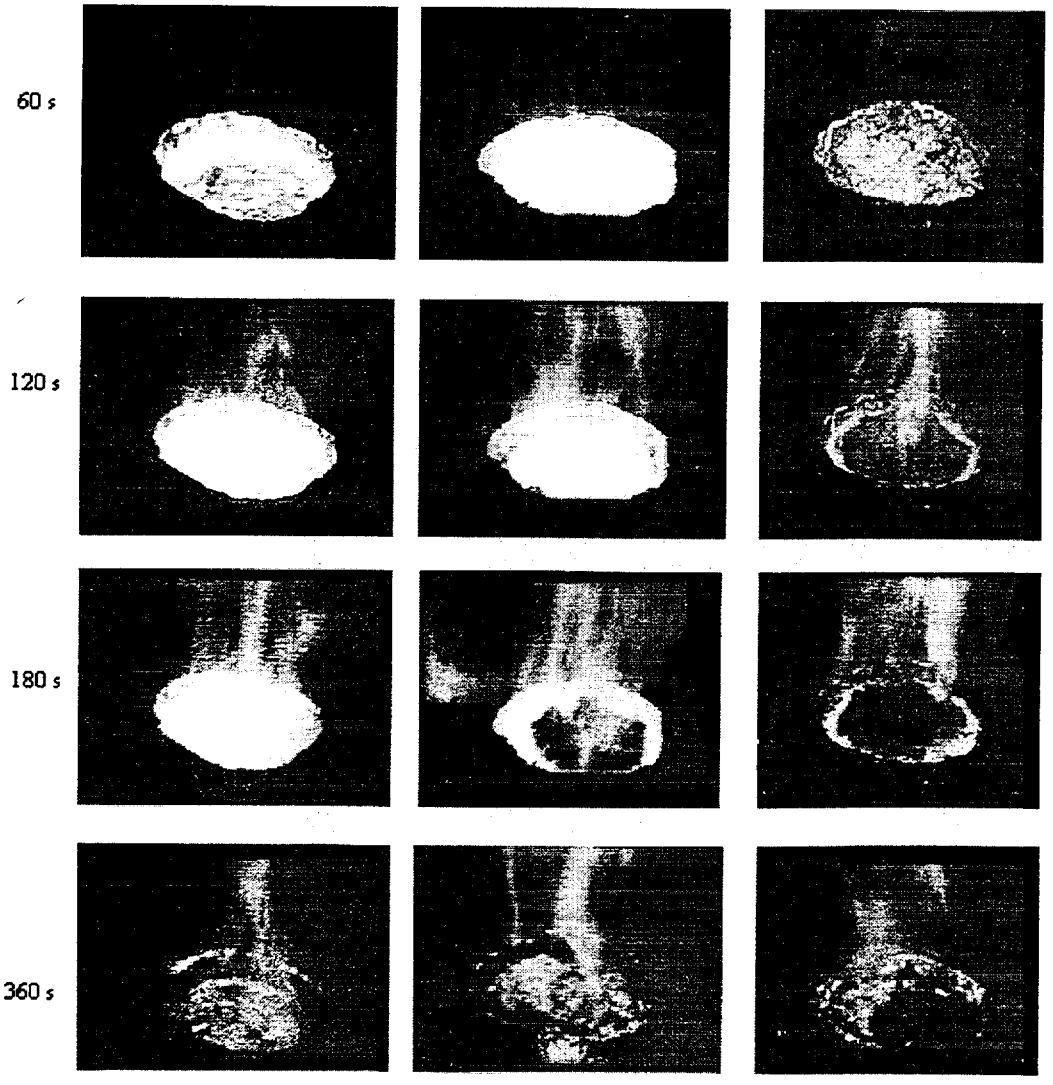

Figure 8. *Images from radiative gasification, at various times, of nylon-6 with N_2 atmosphere (left), nylon-6 clay (5 %) nanocomposite with N_2 atmosphere (center) and nylon-6 clay (5 %) nanocomposite in a N_2/O_2 atmosphere containing a volume fraction of 7.5 % O_2 (right). All samples were exposed to a flux of 40 kW/m^2.*

We have observed similar differences between Cone data and gasification data in another system, the results of which were published previously. In this case the reduction in mass loss rate, due to the presence of silica-additives, in the gasification experiment was only half of that observed in the Cone experiment. However, in this system the residue yield was 15 wt. %

in the Cone and only 9 wt. % in the gasification apparatus[16]. Further study of the possible role of oxygen in the mechanism of flame retardancy for the nanocomposite is underway.

5. VINYL POLYMER NANOCOMPOSITES FLAMMABILITY

Many other polymers have also been prepared as polymer-clay nanocomposites[17]. For the purpose of investigating the general effectiveness of this new approach to flame retarding polymers we have examined the flammability of polymer-clay nanocomposites prepared from polystyrene, PS, and polypropylene-graft-maleic anhydride, PP-g-MA. Like the nylon-6 nanocomposites these polymer-clay nanocomposites are prepared using organic-modified montmorillonite clay. In contrast to the nylon system, these nanocomposites were prepared by the melt blending process[17]. In this process the appropriately modified (compatibilized) montmorillonite clay and the polymer are combined in the melt to form the nanocomposite.

5.1. PS-clay nanocomposite

As described in the experimental section the PS-clay nanocomposite (mass fraction of 3 %) has an *intercalated* structure (see Scheme 1). The inter-gallery spacing, by XRD analysis, is 3.1 nm ($2\theta = 2.7°$).

The HRR data shown in Figure 9 reveals that the *intercalated* nanocomposite, with a mass fraction of only 3 %, has a 45 % lower peak HRR than the *immiscible* PS-clay mixture. The data in Table 1 also shows that the peak HRR for the *intercalated* PS-clay nanocomposite is ~ half of that for *pure* PS as well as for the *immiscible* PS-clay mixture. These data also indicate that, simple mixing the clay into the PS, so that the clay is dispersed like a conventional filler, only to the level of the particle size of the clay (5 μm), is not sufficient to modify the flammability of the PS. Since the HRR of the *immiscible* PS-clay mixture is essentially the same as the HRR for the *pure* PS. It appears that the *intercalated* nano-morphology is necessary for improved flammability. Like the results for nylon-6, the cone data shows that it is the reduced mass loss rate of the *intercalated* PS-clay nanocomposite that is responsible for the improved flammability. Comparison of this Cone data with that for PS flame retarded using decabromodiphenyl oxide, DBDPO, and antimony trioxide, Sb_2O_3, (total mass fraction of 30 %) (Table 1) shows that the *intercalated* nanocomposite results in a similar reduction in the peak HRR for PS, but without as much of an increase in the soot (measured using the specific extinction area, SEA) or CO yields.

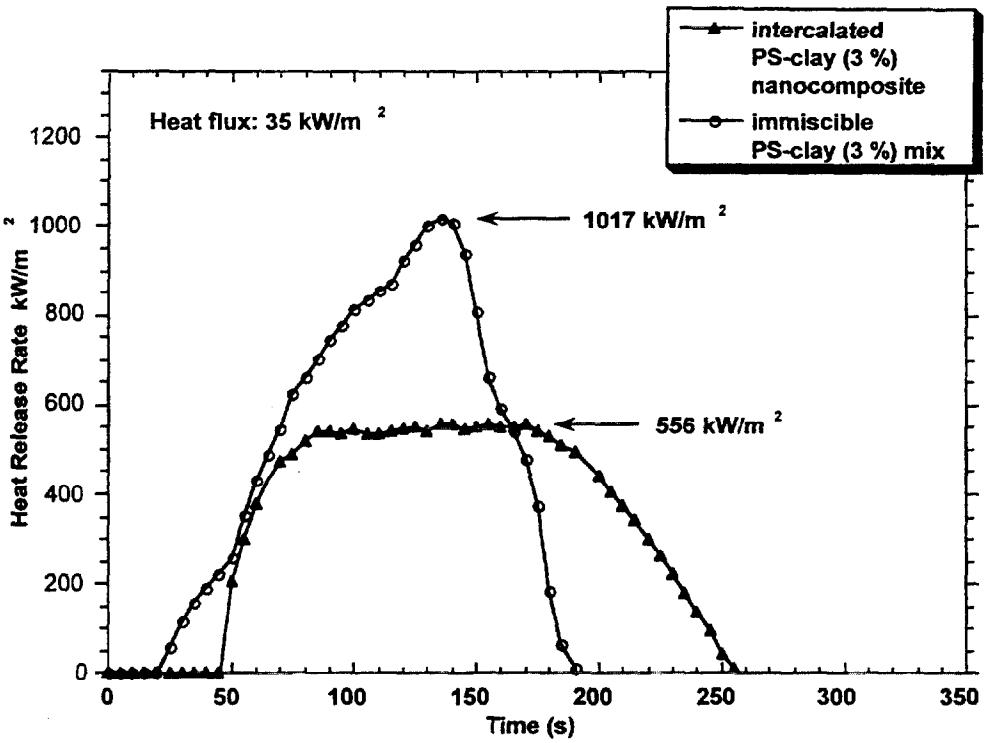

Figure 9. *Heat release rate versus time plot for the intercalated PS-clay nanocomposite and that for the immiscible PS-clay mixture.*

These results were surprising since, the *intercalated* form of the nanocomposite, at such a low clay mass fraction, is inhomogeneous, with *intercalated*-PS-clay domains dispersed in pure PS. The thermal stability of this system is seen in the TGA behavior shown in Figure 10. The TGA of the *intercalated*-PS-clay nanocomposite reveals almost a 50°C increase in the peak for the derivative of the TG plot (DTG) as compared to the peak of the DTG for the *immiscible* PS-clay mixture.

This is in contrast to the nylon-6 clay nanocomposite which showed no change in the peak DTG. Also apparent from the DTG data is the presence of two decomposition peaks for the *intercalated*-PS-clay nanocomposite. The first, at 440°C, coincides with the DTG peak for the *immiscible* PS-clay mixture, the second at 488°C, is most likely from the decomposition of the *intercalated*-PS. Studies, published previously, of the thermal decomposition behavior of several polymer-clay nanocomposites also showed that the *intercalated* form had the highest stability, even greater stability than the *delaminated* nanocomposite[18,19]. We determined that the ratio of the area under the DTG curves for these two decomposition processes is 1.0 to 1.5.

Table 1. *Cone Calorimeter Data*

Sample *(structure)*	Residue Yield (%) ± 0.5	Peak HRR (Δ%) (kW/m^2)	Mean HRR (Δ%) (kW/m^2)	Mean H_c (MJ/kg)	Total Heat Released (MJ/m^2)	Mean Specific Ext. Area (m^2/kg)	Mean CO yield (kg/kg)
Nylon-6	1.0	1,011	603	27	413	197	0.01
Nylon-6 clay-nanocomposite 2% *delaminated*	3.0	686 (32%)	390 (35%)	27	406	271	0.01
Nylon-6 clay-nanocomposite 5% *delaminated*	5.7	378 (63%)	304 (50%)	27	397	296	0.02
PS	0	1,118	703	29	102	1,464	0.09
PS clay- mix 3% *immiscible*	3.2	1,080	715	29	96	1,836	0.09
PS clay-nanocomposite 3% *intercalated*	3.7	567 (48%)	444 (38%)	27	89	1,727	0.08
PS w/ DBDPO/Sb_2O_3 30%	2.6	491 (56%)	318 (54%)	11	38	2,577	0.14
PP-g-MA	0	2,028	861	38	219	756	0.04
PP-g-MA clay nanocomposite 5% *intercalated*	8.0	922 (54%)	651 (24%)	37	179	994	0.05

Hc : Heat of combustion

This indicates that a mass fraction of only 3 % clay in the *intercalated*-PS nanocomposite increases the thermal stability of 60 % of the PS. This ratio was determined using the DTG curve for the *immiscible* PS-clay decomposition to approximate the decomposition contained in the shoulder of the *intercalated*-PS-clay DTG curve. We find that multiplication by the appropriate factor (0.38) gives a ratio of the area under the DTG curves for these two decomposition processes, *immiscible* and *intercalated* respectively, of 1.0 to 1.5. This is in agreement with studies on other polymer-clay nanocomposites where the mass fraction of polymer directly effected by the presence of the clay was found to be ~ 60 %[20].

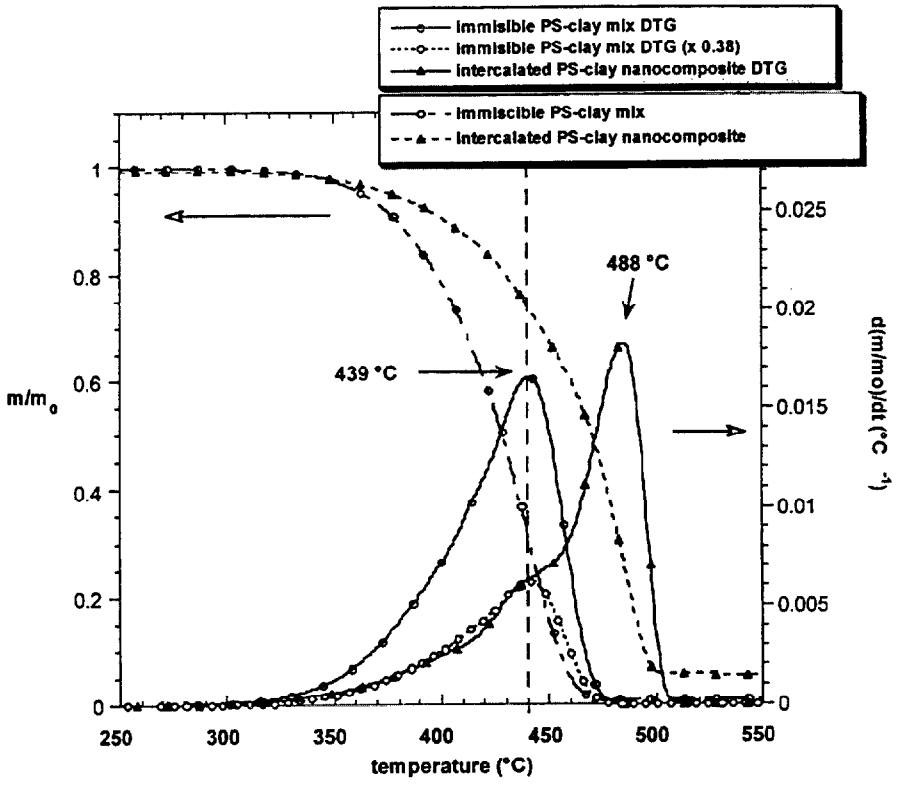

Figure 10. *Normalized TGA plots and DTG plots for immiscible PS-clay (3 %) mixture and intercalated PS-clay (3 %) nanocomposite. The intercalated-PS clay clearly has a greater thermal stability than the immiscible PS-clay mixture.*

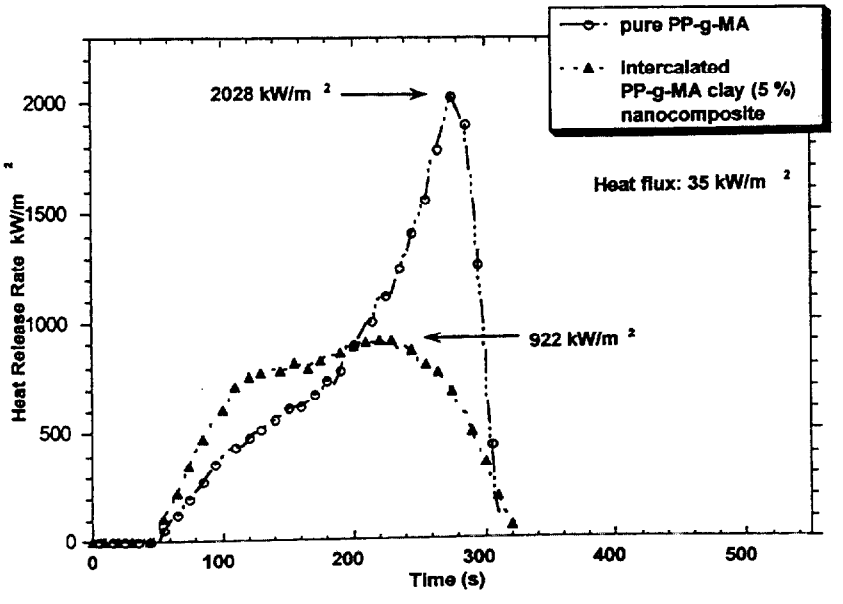

Figure 11. *Heat release rate versus time plot for the intercalated PP-g-MA-clay nanocomposite and that for the pure PP-g-MA.*

5.2. PP-g-MA-clay-nanocomposite

We have also examined the flammability properties of a polypropylene-clay nanocomposite. The PP-g-MA-clay-nanocomposite (clay mass fraction of 5 %) was prepared by melt blending PP-g-MA with bis(dimethyl)bis(tallow)ammonium-exchanged montmorillonite. In this case the melt blending also yielded a nanocomposite with the *intercalated* structure (see Scheme 1). The inter-gallery spacing, by XRD analysis, is 3.6 nm ($2\theta = 2.4°$).

Figure 11 shows that the peak HRR for the *intercalated* PP-g-MA-clay-nanocomposite is 54 % lower than that for pure PP-g-MA. Like the nylon-6 and PS clay nanocomposites, the reduction in HRR for the PP nanocomposite is a direct result of a reduced mass loss rate.

6 SUMMARY

The Cone data in Table 1 shows that the FR performance of the PS-clay nanocomposite and the PP-g-MA-clay nanocomposite is very similar to that for the nylon-6 clay nanocomposite. The Cone data also shows that the FR mechanism for the PS-clay nanocomposite and the PP-g-MA-clay nanocomposite is very similar to that for the nylon-6 clay nanocomposite. That is, the heat of combustion, and rates of soot and CO formation are unchanged, within the experimental uncertainty, by the presence of the clay in the nylon-6, PS and PP nanocomposites. Furthermore, the residue yields from combustion, for all the polymer, are not high enough to account for the reduced flammability due to retention of carbon in the condensed phase. A condensed phase mechanism where a reinforced char layer forms, which acts as an insulator and a mass transport barrier, slowing the escape of the volatile decomposition products generated as the polymer decomposes appears to be one likely explanation for the excellent FR performance of the clay-nanocomposites.

References

1. G. L. Nelson, *"Fire and Polymers II"*, *ACS Symposium Series* 599, ed. G. L. Nelson, American Chemical Society, Washington, DC, pp. 1-28 (1995).
2. S. Levchik, G. Camino, L. Costa, and G. Levchik, *Fire and Materials*, **19**, 1 (1995).
3. A. Hochberg, *"Proceedings of the Fall FRCA Meeting"*, Naples, FL., 159 (1996).
4. Y. Kojima, A. Usuki, M. Kawasumi, A. Okada, Y. Fukushima, T. Kurauchi, and O. Kamigaito, *J. Mater. Res.*, **8**, 1185 (1993).
5. J. W. Gilman, T. Kashiwagi, J. D. Lichtenhan, *SAMPE Journal*, **33(4)**, 40 (1997).
6. V. Babrauskas, R. Peacock, *Fire Safety Journal*, **18**, 255 (1992).

7. V. Babrauskas, *Fire and Materials*, **19**, 243 (1995).
8. Certain commercial equipment, instruments, materials, services or companies are identified in this paper in order to specify adequately the experimental procedure. This in no way implies endorsement or recommendation by NIST.
9. A. Usuki, Y. Kojima, M. Kawasumi, A. Okada, Y. Fukushima, T. Kurauchi, and O. Kamigaito, *J. Mater. Res.*, **8**, 1179 (1993).
10. V. Babrauskas, R. Peacock, *Fire Safety Journal*, **18**, 255 (1992).
11. A. Grand, *SAMPE Journal*, **33(4)**, 47 (1997).
12. R. Harris, Jr., V. Babrauskas, B. C. Levin and M. Paabo, NISTR 4649, 1991.
13. J. M. Thomas, "*Intercalation Chemistry,* Chapter 3", Academic Press Inc., London, 1982, p. 55.
14. E. Giannelis, and P. Messersmith, *J. Polym. Sci. A: Polym. Chem.*, **33**, 1047 (1995).
15. M. Nyden, J. W. Gilman, "*Computational and Theoretical Polymer Science*", in press, 1998.
16. J. Gilman, S. Ritchie, T. Kashiwagi, and S. Lomakin, *Fire and Materials*, **21**, 23 (1997).
18. E. Giannelis, *Adv. Mater.*, **8**, 29 (1996).
19. J. Lee, T. Takekoshi and E. Gannelis, *Mat. Res. Soc. Symp. Proc.*, **457**, p. 513, (1997).
20. J. Lee and E. Giannelis, *Polymer Preprints*, **38**, 688, (1997).
21. S. Burnside, *Ph. D. Thesis*, Cornell University, 1997.

Acknowledgements

The authors would like to thank the Federal Aviation Administration for partial funding of this work, through Interagency Agreement DTFA0003-92-Z-0018. We would also like to thank Mr. Michael Smith for Cone Calorimeter analysis, Lori Brassel for TGA analysis, Dr. Catheryn Jackson and Dr. Henri Chanzy for TEM analysis of the char samples, Dr. Marc Nyden for the montmorillonite structure. We would also like to express our gratitude to Dow Chemical Co. for PS samples (STYRON 6127), Ube America Inc. for nylon-6 clay nanocomposite samples and Southern Clay Products for the organic-modified clays, Closite 15A and 3A.